

## Identification of a Nonpeptidic and Conformationally Restricted Bradykinin B1 Receptor Antagonist with Anti-Inflammatory Activity

Derin C. D'Amico,<sup>\*,†</sup> Toshi Aya,<sup>†</sup> Jason Human,<sup>†</sup> Christopher Fotsch,<sup>†</sup> Jian Jeffrey Chen,<sup>†</sup> Kaustav Biswas,<sup>†</sup> Bobby Riahi,<sup>†</sup> Mark H. Norman,<sup>†</sup> Christopher A. Willoughby,<sup>†,‡</sup> Randall Hungate,<sup>†</sup> Paul J. Reider,<sup>†</sup> Gloria Biddlecome,<sup>§</sup> Dianna Lester-Zeiner,<sup>§</sup> Carlo Van Staden,<sup>§</sup> Eileen Johnson,<sup>||</sup> Augustus Kamassah,<sup>||</sup> Leyla Arik,<sup>||</sup> Judy Wang,<sup>||</sup> Vellarkad N. Viswanadhan,<sup>⊥</sup> Robert D. Groneberg,<sup>#</sup> James Zhan,<sup>#</sup> Hideo Suzuki,<sup>#</sup> Andras Toro,<sup>#</sup> David A. Mareska,<sup>#</sup> David E. Clarke,<sup>#</sup> Darren M. Harvey,<sup>#</sup> Laurence E. Burgess,<sup>#</sup> Ellen R. Laird,<sup>#</sup> Benny Askew,<sup>⊗</sup> and Gordon Ng<sup>○</sup>

Chemistry Research and Development, Neuroscience, HTS/Molecular Pharmacology, Molecular Structure and Design, and Inflammation, Amgen Inc., One Amgen Center Drive, Thousand Oaks, California 91320, and Array BioPharma, 3200 Walnut Street, Boulder, Colorado 80301

Received October 19, 2006

**Abstract:** We report the discovery of chroman **28**, a potent and selective antagonist of human, nonhuman primate, rat, and rabbit bradykinin B1 receptors (0.4–17 nM). At 90 mg/kg s.c., **28** decreased plasma extravasation in two rodent models of inflammation. A novel method to calculate entropy is introduced and ascribed ~30% of the gained affinity between “flexible” **4** ( $K_i = 132$  nM) and “rigid” **28** ( $K_i = 0.77$  nM) to decreased conformational entropy.

Kinins (bradykinin-related peptides) are potent vasoactive molecules implicated in inflammation and pain that mediate their acute and chronic actions via bradykinin receptors, which are either constitutively expressed (B2) or inducible (B1).<sup>1,2</sup> The B2-antagonist icatibant (HOE-140) is being developed as an anti-inflammatory agent for osteoarthritis.<sup>3</sup> While rodent hypertension following systemic HOE-140 administration has been observed,<sup>4</sup> it is unclear whether this effect would limit human use. A phase II clinical trial looking at the effects of HOE-140 following intra-articular injection (into the knee) was initiated. The route of administration *may* have been chosen, among other factors, to mitigate potential B2-related hypertensive effects. Reports of B1 antagonists in the clinic, however, are not available. The preclinical role of B1 signaling in inflammation,<sup>5,6</sup> pain,<sup>6</sup> edema, and loss of function<sup>7</sup> has been described. Of relevance to our *in vivo* models (*vide infra*), B1-knockout mice lacked the B1-agonist-induced plasma extravasation (edema) response observed in their wild-type litter mates. Based on these results, a B1-selective antagonist would be useful as an anti-inflammatory agent.

\* To whom correspondence should be addressed. Amgen, Inc., One Amgen Center drive, MS-B29-4-2-D, Thousand Oaks, California 91320. Tel.: 805-447-7354. Fax: 805-480-3016. E-mail: ddamico@amgen.com.

<sup>†</sup> Chemistry Research and Development, Amgen, Inc.

<sup>‡</sup> Deceased (12/31/2002).

<sup>§</sup> HTS/Molecular Pharmacology, Amgen, Inc.

<sup>||</sup> Neuroscience, Amgen, Inc.

<sup>⊥</sup> Molecular Structure and Design, Amgen, Inc.

<sup>#</sup> Array BioPharma.

<sup>⊗</sup> Current address: Serono Research Institute, Rockland, MA.

<sup>○</sup> Inflammation, Amgen, Inc.

A major drawback for the preclinical assessment of human B1 (hB1) antagonists is the cross-species divergence in pharmacology and, in particular, between human and rodent. Transgenic rats<sup>8</sup> expressing the human receptor have been used to address interspecies differences in B1 pharmacology. While useful, *in vivo* results derived from humanized rat studies are *potentially* complicated by the physiologically regulated rodent B1 (rB1) receptor expressed in the background. A preferred approach to drug development is to conduct target validation studies with an agent that is active across species. Indeed, there are reports of B1 antagonists with comparable potencies against rB1 and hB1 receptors. For example, researchers at Sanofi published a series of dipeptoid sulfonamides such as **1**<sup>9</sup> (Figure 1, hB1  $K_i = 0.48$  nM; rat ileum  $pA_2 = 9.4$ ). Additionally, scientists at Merck disclosed two series<sup>10,11</sup> that are essentially equipotent at both hB1 and rB1 receptors. Ultimately, the need for potency at nonprimate receptors is required to establish preclinical *in vivo* efficacy. Accordingly, our goal was to identify novel, selective, and potent hB1 antagonists with *sufficient* rB1 potency and pharmacokinetic properties to demonstrate anti-inflammatory efficacy in a rodent model of inflammation.

The majority of small molecule B1 antagonists have a basic amine and a lipophilic sulfonamide as exemplified by R<sub>1</sub> and R<sub>2</sub> (**1**, Figure 1), an observation also noted by Marceau.<sup>12</sup> The requirement for a basic residue probably stems from a favorable interaction with either of the two acidic residues within extracellular domain 4 (EC<sub>4</sub>), namely, Glu<sup>273</sup> or Asp<sup>291</sup>. In addition, EC<sub>4</sub> has been shown to be important for species-specific pharmacology.<sup>11</sup> Initial lead identification efforts sought to optimize the spatial placement between a basic amine (R<sub>3</sub>) and the 2-naphthylsulfonamide (R<sub>4</sub>) of  $\beta$ -phenylalanine. From these investigations, compound **2** was identified as a moderately potent antagonist of the hB1 receptor (IC<sub>50</sub> = 359 nM) as determined by a B1-mediated calcium mobilization assay. Furthermore, compound **2** had excellent selectivity over the B2 subtype (hB1  $K_i = 382$  nM vs hB2  $K_i = 56\,000$  nM). Subsequent studies showed that **4**-(R) contained the activity observed with **2** (hB1  $K_i = 132$  nM (SEM = 16 nM,  $n = 4$ ); hB1 IC<sub>50</sub> = 447 nM); **3**-(S) was devoid of functional potency up to 4000 nM. A second lead, compound **6** (IC<sub>50</sub> = 520 nM), was obtained by extending the distance from the sulfonamide to the basic amine by one methylene unit. With these leads in hand, efforts to improve potency were initiated.

One strategy that has been successfully used by medicinal chemists to increase potency for a given receptor involves decreasing the flexibility of a lead compound.<sup>13</sup> In doing so, the entropic penalty associated with adopting a preferred binding conformation is minimized. Accordingly, the benzylic position of **4** was “fixed” to the arene ring via a six-membered carbocycle. The resulting tetralin **5** was ~75-fold more potent (hB1 IC<sub>50</sub> = 6 nM) than the acyclic **4**. Interestingly, when a similar cyclization was applied to phenethylamine **6** (to afford bicycle **7**), a modest increase in potency was observed (IC<sub>50</sub>: 570 nM → 380 nM). This communication reports the synthesis and biological evaluation of a series of constrained analogs such as tetralin **5**.

Compounds **2–4** were prepared as shown in Scheme 1. Monoprotected diamine **8** was alkylated with 1,5-dibromopentane to give piperidine **9**. The Boc protecting group was removed and the resulting amine, **10**, was coupled with ( $\pm$ )-**11**

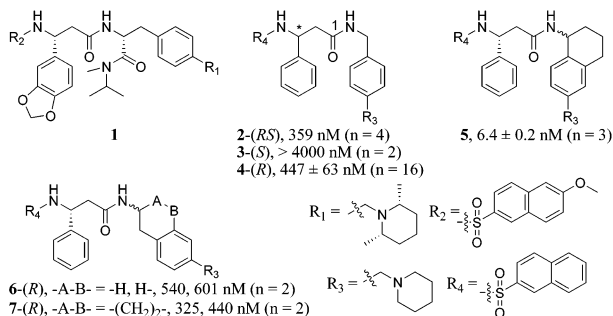
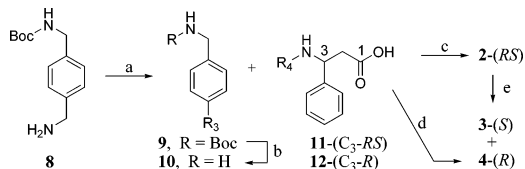


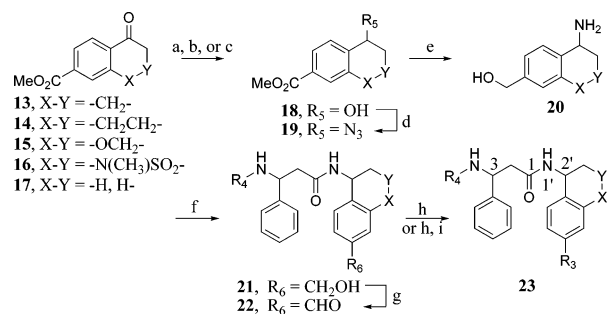
**Figure 1.** hB1 antagonists and their associated potencies (IC<sub>50</sub> ± SEM).

**Scheme 1<sup>a,b</sup>**



<sup>a</sup> Reagents and conditions: (a) Br(CH<sub>2</sub>)<sub>5</sub>Br, K<sub>2</sub>CO<sub>3</sub>, CH<sub>3</sub>CN; (b) HCl, MeOH; (c) **11**, HOBT, EDC, DMF; (d) **12**, HOBT, EDC, DMF; (e) Chiralcel OJH, *ee* > 99.5%. <sup>b</sup>R<sub>3</sub> and R<sub>4</sub> are defined in Figure 1.

**Scheme 2<sup>a,b</sup>**



<sup>a</sup> Reagents and conditions: (a) (*R*)-CBS, toluene, -10 °C; (b) NaBH<sub>4</sub>, MeOH; (c) (*S*)-CBS, toluene, -10 °C; (d) DPPA, toluene, 0 °C → room temperature; (e) LiAlH<sub>4</sub>, THF, -15 °C; (f) **11** or **12**, Si-DCC, NHS, THF-CH<sub>2</sub>Cl<sub>2</sub>; (g) MnO<sub>2</sub>, CH<sub>2</sub>Cl<sub>2</sub>; (h) piperidine, NaB(OAc)<sub>3</sub>H, HOAc, DCE; (i) Chiralcel OJH, *de* and *ee* > 99.5%. <sup>b</sup>R<sub>3</sub> and R<sub>4</sub> are defined in Figure 1.

to afford amide **2** as a racemic mixture. This mixture was separated using chiral supercritical fluid chromatography (c-SFC) to afford analogs **3** and **4** with >99% *ee*. Comparison of the retention times (from c-SFC) of the separated enantiomers with that of **4** (from chiral acid **12**) proved that the *R*-form contained the hB1 potency in racemic amide **2**.

The synthesis of the constrained analogs, such as **5**, required the preparation of a series of novel bicyclic amines (Scheme 2). Known ketones **13**–**17** were reduced either with NaBH<sub>4</sub> to afford racemic alcohols **18** or with Corey–Bakshi–Shibata<sup>14</sup> (CBS) conditions to give the corresponding chiral alcohols **18**. The (*S*)-alcohols were synthesized using (*D*)-leucine as the chiral auxiliary in the CBS reduction ((*R*)-CBS), whereas the (*R*)-alcohols were synthesized with (*L*)-leucine as the chiral controller ((*S*)-CBS). The enantiomeric purities were 96–98%, as determined by c-SFC analysis. Conversion of the hydroxyl groups into azides **19** with stereochemical inversion was accomplished using diphenylphosphoryl azide (DPPA).<sup>15</sup> No detectable loss of enantiomeric purity (via c-SFC) was observed in the conversion of **18** → **19**. Both the azido- and ester- groups were reduced with LiAlH<sub>4</sub> to afford the corresponding amino alcohols **20**. To confirm the stereochemical outcome of the sequence, an X-ray study was conducted on a representative example. Specifically, crystals of aminotetralinol **20** (X–Y =

**Table 1**

cmpd	X–Y	C <sub>2</sub> ' C <sub>3</sub>	binding K <sub>i</sub> , mean (SEM)		hB1 IC <sub>50</sub> , nM mean (SEM)
			hB1	hB2	
<b>24</b>	–CH <sub>2</sub> –	R R	1.6 (0.7) <sup>a</sup>	49 200 (600) <sup>b</sup>	5.6 (0.7) <sup>c</sup>
<b>25</b>	–CH <sub>2</sub> –	S R	241, 327	13 300 (1000) <sup>b</sup>	183 (2) <sup>a</sup>
<b>26</b>	–CH <sub>2</sub> CH <sub>2</sub> –	R R	0.24 (0.03) <sup>c</sup>	57 000 (1600) <sup>b</sup>	5.5 (0.7) <sup>g</sup>
<b>27</b>	–CH <sub>2</sub> CH <sub>2</sub> –	S R	31, 39	15 000 (1300) <sup>c</sup>	86 (6) <sup>a</sup>
<b>28</b>	–OCH <sub>2</sub> –	R R	0.77 (0.06) <sup>f</sup>	> 50 000 <sup>i</sup>	3.4 (0.1) <sup>j</sup>
<b>29</b>	–OCH <sub>2</sub> –	S R	17 (4) <sup>b</sup>	> 20 000 <sup>g</sup>	418 (89) <sup>e</sup>
<b>30</b>	–OCH <sub>2</sub> –	R S	144, 143	ND	519 (85) <sup>c</sup>
<b>31</b>	–OCH <sub>2</sub> –	S S	1900, 2900	ND	1700 (300) <sup>a</sup>
<b>32</b>	–N(CH <sub>3</sub> )SO <sub>2</sub> –	S R	15.80, 15.87	16 000 (1000) <sup>b</sup>	14 (0.4) <sup>a</sup>
<b>33</b>	–N(CH <sub>3</sub> )SO <sub>2</sub> –	R R	1.3, 1.5	35 000 (3500) <sup>b</sup>	10.7 (0.2) <sup>a</sup>
<b>34</b>	–H, H–	R R	17 (4) <sup>a</sup>	ND	302 (45) <sup>d</sup>

<sup>a</sup> Number of measurements (NM): 4. <sup>b</sup> 4 NM: 7. <sup>c</sup> 12 NM: 16. <sup>d</sup> 16 NM: 24. <sup>e</sup> 24 NM: 31. <sup>f</sup> 31 NM: 48. <sup>g</sup> 48 NM: 248. <sup>h</sup> 248 NM: 1118. <sup>i</sup> 1118 NM: 9188.

–CH<sub>2</sub>CH<sub>2</sub>–) were obtained from THF–MTBE, which afforded high quality diffraction data. Using the method of Flack,<sup>16</sup> it was possible to assign the (*R*)-configuration to the single stereocenter. This conclusion verified that the (*R*)-CBS reduction produced the expected (*S*)-tetralin alcohol and that a single inversion was realized in the **18** → **19** sequence. Amines **20** were coupled with either acid **11** or **12** using silica-supported carbodiimide (Si–DCC) and *N*-hydroxysuccinimide (NHS) to afford amides **21**. Manganese dioxide oxidation of benzylic alcohols **21** afforded aldehydes **22** in good yield, which when treated with piperidine/NaB(OAc)<sub>3</sub>H/HOAc, afforded amines **23**. Diastereomeric mixtures of **23** were separated at this point using preparative c-SFC. Without exception, the tested compounds shown in Table 1 were obtained with >99% *de*, *ee*, and purity.

The binding affinities for the hB1 and hB2 receptor subtypes were next determined for the new analogs (Table 1). Tetralin **26** and chroman **28** showed the highest affinity for hB1 (K<sub>i</sub> = 0.24 and 0.77 nM, respectively) and selectively bound this subtype with >10<sup>5</sup> orders of magnitude over the hB2 receptor. These cyclic analogs had affinities that were significantly (*p* < 0.01) lower than the acyclic **4** (K<sub>i</sub> = 132 nM), as determined by Student's *t*-test at the 95% confidence level. Subsequent studies attribute this 170- to 550-fold affinity gain primarily to enthalpic factors and secondarily to decreased conformational entropy (vide infra). Because a high degree of selectivity over hB2 was uniformly achieved, subsequent biological discussions will focus on hB1 functional potency using the calcium flux assay.

In this SAR study, the structural variables examined were the polarity and conformational flexibility of the analogs and the configuration present at C<sub>2</sub>' and C<sub>3</sub>. The most potent compounds were tetralin **26**, chroman **28**, indane **24**, and sultams **32** and **33** (hB1 IC<sub>50</sub> = 3–14 nM). The polarity within these five analogs varied between sultam **32** and tetralin **26** (Δ*c*Log*P* = 1.4), which when plotted against their associated potencies, hinted at a correlation between lipophilicity and potency. Development of this SAR was ended, because the potencies of sultam **32** and tetralin **26** were statistically equivalent (Student's *t*-test at 95% confidence). A significant difference (*p* < 0.0001), however, was observed between the acyclic (**2**, **4**, and **34**) and cyclic compounds (**24**, **26**, **28**, **32**, and **33**); Chroman **28** was 125-fold more potent than the initial lead, compound **4**. The strategy to increase activity relative to compound **4**, therefore, was successful as five potent analogs were identified (IC<sub>50</sub> < 14 nM).

One consequence of the conformational-restriction strategy was the generation of an additional stereocenter at C<sub>2</sub>' (as in **23**, Scheme 2), which when coupled to the center at C<sub>3</sub> afforded

four possible diastereomers. The  $C_2'$ -(*R*) and  $C_3$ -(*R*) isomers proved to be the optimal configuration for potency in each of the ring systems (i.e., **24**, **26**, **28**, and **33**). However, there was no preference for  $C_2'$ -(*R*) in the sultam series; the  $C_2'$ -(*S*) diastereomer, **32**, was equipotent to **33**. This finding contrasts the trend observed in the indane, tetralin, and chroman analogs; activity decreased by 16- to 100-fold when  $C_2'$  was changed from (*R*) to (*S*). The statistically significant rank order of potency as a function of both  $C_2'$  and  $C_3$  was  $RR > SR > RS > SS$  (i.e., **28** > **29** > **30** > **31**). The (*S*)-configuration, whether at  $C_2'$  or  $C_3$ , resulted in decreased potency.

Studies in B1-transfected CHO cells showed that chroman **28** had comparable potency ( $IC_{50} \pm SEM$  (n)) at the human ( $3.4 \pm 0.1$  nM (1118)), rabbit ( $17 \pm 4$  nM (10)) rat- ( $4 \pm 1$  nM (8)), and African green monkey B1 receptors ( $0.40 \pm 0.02$  nM (17)). Additionally, the compound prevented a B1 agonist-induced (*Lys-desArg*<sup>9</sup>-BK) contraction of isolated human umbilical vein with a  $pA_2 = 7.4$  (40 nM; Supporting Information, section 3e). Having obtained rB1 potency, the rodent pharmacokinetic properties of chroman **28** were measured (Supporting Information, section 4a). Compound **28** had an apparent clearance (Cl/F) of 5 L when dosed intravenously (i.v.) or subcutaneously (s.c.), a plasma fraction unbound ( $f_{ub}$ ) of 0.032 and a s.c. bioavailability of 100%. Taken together, plasma levels in excess of the presumed pharmacologically relevant drug concentration ( $IC_{50}/f_{ub} = 125$  nM) could be obtained for 5–6 h following a 90 mg/kg s.c. dose.

Chroman **28** was studied in the rat pleurisy and the reverse passive Arthus (RPA) models of inflammation. Both models afford the same endpoint, namely, plasma extravasation (edema) within the pleural cavity, but differ in the way the inflammation is initiated. Carrageenan was used in the pleurisy model and rabbit IgG complexation to goat anti-rabbit IgG was used in the RPA model. The latter model is thought to mimic an immune-based inflammatory condition but without engaging the host's immune system. Chroman **28** (90 mg/kg, s.c.) reduced the collected exudate by 22% relative to control (Dunnett's method,  $p = 0.0003$ , Supporting Information, section 4b, vii–viii). The unbound-drug concentration for the 90 mg/kg cohort was  $169 \pm 15$  nM (SEM,  $n = 8$ , Supporting Information, section 4b, ix). As a control, the Cox-1/2 inhibitor indomethacin (Indo) was administered at the highest dose not associated with gastric bleeding (3 mg/kg *per oral*, p.o.). As observed for chroman **28**, Indo reduced edema formation by 28% ( $p < 0.0001$ ). In the RPA model, reduction in exudate volume was observed at 30 (14%,  $p = 0.0002$ ), 60 (10%,  $p = 0.005$ ), and 90 mg/kg (26%,  $p < 0.0001$ ) relative to saline treated animals (Supporting Information, section 4c, vi–vii). The responses observed at the 30 and 60 mg/kg doses were not statistically different from each other. Indo at 3 mg/kg p.o., however, was without effect in the RPA model. Apparently, the two models afford distinct inflammatory states, one that is Indo-sensitive (pleurisy) and one that is Indo-insensitive (RPA). Unlike Indo, chroman **28** was efficacious in both models.

To better understand the reasons for the 550-fold increase in  $K_i$  (**4** → **26**), and to aid the development of a pharmacophore model, a computational study was performed. Entropy is often used to rationalize the increased affinity associated with the receptor binding of more- versus less-rigid ligands; flexible molecules can exist in more distinct conformations and, therefore, the probability of existing in any one (i.e., the receptor-preferred conformer) is lower than that of a rigid molecule. Surprisingly, the literature provided no examples that have *quantitatively* measured the entropic component in a

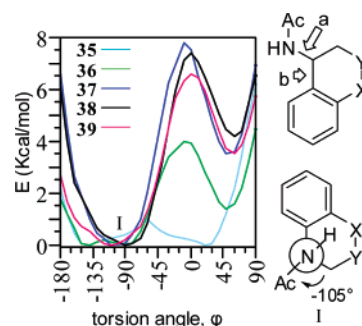


**Figure 2.** Energy profiles and Newman projection (I) about torsion “a” for **35–39**.

ligand–receptor binding event. Herein, we describe a method that uses Shannon entropy,<sup>17</sup> an equation that has been used to characterize protein<sup>18</sup> and polymer conformations.<sup>19</sup> The affinities for two acyclic analogs, **4** and **34**, along with those of the cyclic analogs **24**, **26**, and **28** formed the basis set for an ab initio study. To simplify the calculations, the following structural approximations were used: **4** ≈ *N*-acetylbenzylamine (**35**), **34** ≈ *N*-acetyl- $\alpha$ -methylbenzylamine (**36**), **24** ≈ *N*-acetyl-2-aminoindane (**37**), **26** ≈ *N*-acetyl-2-aminotetralin (**38**), and **28** ≈ *N*-acetyl-2-aminochroman (**39**). The calculations showed the rotational freedom about bond “a” (Figure 2) was restricted in the bicyclic ring systems **37–39** and, to a lesser extent, in the methyl-substituted benzylamine **36**. Specifically, cyclic analogs **37–39** had two gas-phase minima separated by 3.5 kcal mol<sup>-1</sup> energy located at  $-105^\circ$  (Figure 2, I) and  $-60^\circ$ . The acyclic **36** likewise contained two minima, but with a diminished  $\Delta E$  (1.5 kcal mol<sup>-1</sup>). The two minima observed in **36–39** became degenerate in compound **35** (minima at  $-150^\circ$  and  $30^\circ$ ) due to symmetry ( $\sigma$ ).

The conformational entropy for **35–39** was next calculated by converting their respective energy profiles (Figure 2) into probability functions (eq 1). The entropy term,  $T\Delta S$ , was obtained by applying the Shannon relationship (eq 2) to the derived probability functions.

$$p_{\varphi_i} = e^{(-E_{\varphi_i}/kT)} / \sum_i e^{(-E_{\varphi_i}/kT)} \quad (1)$$

$$T\Delta S = RT(-\sum_i p_{\varphi_i} \ln[p_{\varphi_i}]) \quad (2)$$

$$\text{BFE} = RT(\text{Ln}(hB1K_i)) \quad (3)$$

where  $p_{\varphi_i}$  is the probability that a molecule lies with a dihedral angle  $\varphi$ ,  $E_{\varphi_i}$  is the energy for that state,  $R$  is the universal gas constant (1.987 cal mol<sup>-1</sup> K<sup>-1</sup>),  $T$  is temperature in Kelvin,  $K_i$  is the affinity in moles L<sup>-1</sup>, and BFE is the binding free energy. This method calculates the total number of conformations a molecule can exist in by integrating the probability that a molecule will exist in a conformation with angle  $\varphi$ , within the limits  $\varphi = 0$  to  $360^\circ$ . Using this approach on otherwise equivalent compounds, it can be shown that a molecule with a single, narrow energy well would have a lower calculated  $T\Delta S$  than one with several accessible minima or one that has a single, wide energy well.

The calculated  $T\Delta S$  (kcal mol<sup>-1</sup>) for **35–39** as a function of the “a” bond were (in decreasing order):  $T\Delta S_{35F(a)} = 1.82$ ;  $T\Delta S_{36F(a)} = 1.52$ ;  $T\Delta S_{37F(a)} = 1.38$ ;  $T\Delta S_{39F(a)} = 1.29$ ; and  $T\Delta S_{38F(a)} = 1.22$ . These data correlated well with the increased affinity observed for their corresponding full structures (**4** > **34** > **24** > **28** > **26**,  $r^2 = 0.97$ , for plots see Supporting Information 2c). The exceptional linearity is hard to ignore because it is statistically significant ( $p = 0.0025$ ). However,



because the hB1 binding assay did not differentiate between analogs **24**, **26**, and **28**, the danger of overinterpretation exists. There was a significant difference between the cyclic and the acyclic analogs (i.e., **26** and **4**, vide supra), and therefore, the change in BFE for tetralin **26** relative to **4** is significant ( $\Delta\text{BFE}_{26\text{F}(4)} = \text{BFE}_{26} - \text{BFE}_4 = 3.7 \text{ kcal mol}^{-1}$ ). The entropy term of  $\Delta\text{BFE}_{26\text{F}(4)}$  was  $-0.6 \text{ kcal mol}^{-1}$  ( $T\Delta S_{38\text{F}(a)} - T\Delta S_{35\text{F}(a)}$ ) or about 20% of the 550-fold gain in affinity. While relevant to SAR pertaining to bond “a”, the value for  $T\Delta S_{35\text{F}(a)}$  underestimates the total entropic effect because it does not include the contributions due to bond “b” (Figure 2). Taking into account both bonds afforded  $T\Delta S_{35\text{F}(a,b)} = 2.3 \text{ kcal mol}^{-1}$ , which decreased the change in entropy for **35**  $\rightarrow$  **38** to  $-1.1 \text{ kcal mol}^{-1}$  ( $\Delta(T\Delta S_{38\text{F}(a,b)}) = T\Delta S_{38\text{F}(a)} - T\Delta S_{35\text{F}(a,b)}$ ). To put the numbers into perspective, a  $1.1 \text{ kcal mol}^{-1}$  decrease in entropy corresponds to an  $\sim 7$ -fold increase in affinity; it is not the major factor behind the 550-fold gain. Enthalpy ( $\Delta\Delta H_{26\text{F}(4)}$ ), on the other hand, accounted for  $2.6 \text{ kcal mol}^{-1}$  of the  $3.7 \text{ kcal mol}^{-1}$  increase in  $\Delta\text{BFE}_{26\text{F}(4)}$  ( $\Delta\Delta H_{26\text{F}(4)} = \Delta\text{BFE}_{26\text{F}(4)} + \Delta(T\Delta S_{38\text{F}(a,b)})$ ). The presence of favorable enthalpic interactions (e.g., Van der Waals) between the atoms required to make the cycle (X–Y, Figure 2) and the receptor are the primary factor underlying the affinity gain between acyclic **4** ( $K_i = 132 \text{ nM}$ ) and cyclic **26** ( $K_i = 0.24 \text{ nM}$ ). Decreased conformational flexibility, while significant, contributed  $\sim 30\%$  of the BFE difference between the two molecules.

In summary, chroman **28** was identified as a potent B1-selective antagonist with in vitro activity across multiple species and anti-inflammatory activity in vivo. A computational study suggested that while decreased conformational entropy correlated with increased affinity, favorable enthalpic interactions between the atoms required to make the molecule more rigid and the receptor accounted for the 550-fold affinity enhancement (**4**  $\rightarrow$  **26**). Finally, it should be noted that potent hB1 antagonists occupied conformation I (Figure 2,  $\varphi = -105 \pm 25^\circ$ )  $> 90\%$  of the time. It seems likely that this orientation lies close to the receptor-preferred binding conformation.

**Acknowledgment.** The authors express our gratitude to M. P. Seed, S. K. McMaster, and D. A. Willoughby for conducting the in vivo assays. Additionally, the reviewer’s comments were helpful, thought-provoking, and very much appreciated.

**Supporting Information Available:** Detailed biological methods and results, synthetic experimentals, and computational data and methodologies (61 pages). This material is available free of charge via the Internet at <http://pubs.acs.org>.

## References

- Dray, A.; Perkins, M. Bradykinin and inflammatory pain. *Trends Neurosci.* **1993**, *16* (3), 99–104.
- Proud, D.; Kaplan, A. P. Kinin formation: Mechanisms and role in inflammatory disorders. *Annu. Rev. Immunol.* **1988**, *6* (1), 49–83.
- Carini, F.; Guelfi, M.; Lecci, A.; Tramontana, M.; Meini, S.; Giuliani, S.; Montserrat, X.; Pascual, J.; Fabbri, G.; Ricci, R.; Quartara, L.; Maggi, C. A. Cardiovascular effects of peptide kinin B2 receptor antagonists in rats. *Can. J. Physiol. Pharmacol.* **2002**, *80* (4), 310–322.
- Carini, F.; Guelfi, M.; Lecci, A.; Tramontana, M.; Meini, S.; Giuliani, S.; Montserrat, X.; Pascual, J.; Fabbri, G.; Ricci, R.; Quartara, L.; Maggi, C. A. Cardiovascular effects of peptide kinin B2 receptor antagonists in rats. *Can. J. Physiol. Pharmacol.* **2002**, *80* (4), 310–322.
- Pesquero, J. B.; Araujo, R. C.; Heppenstall, P. A.; Stucky, C. L.; Silva, J. A., Jr.; Walther, T.; Oliveira, S. M.; Pesquero, J. L.; Paiva, A. C. M.; Calixto, J. B.; Lewin, G. R.; Bader, M. Hypoalgesia and altered inflammatory responses in mice lacking kinin B1 receptors. *Proc. Natl. Acad. Sci. U.S.A.* **2000**, *97* (14), 8140–8145.
- Ferreira, J.; Beirith, A.; Mori, M. A. S.; Araujo, R. C.; Bader, M.; Pesquero, J. B.; Calixto, J. B. Reduced nerve injury-induced neuropathic pain in kinin B1 receptor knock-out mice. *J. Neurosci.* **2005**, *25* (9), 2405–2412.
- Sharma, J. N.; Buchanan, W. W. Pathogenic responses of bradykinin system in chronic inflammatory rheumatoid disease. *Exp. Toxicol. Pathol.* **1994**, *46* (6), 421–33.
- Hess, J. F.; Ransom, R. W.; Zeng, Z.; Chang, R. S. L.; Hey, P. J.; Warren, L.; Harrell, C. M.; Murphy, K. L.; Chen, T.-B.; Miller, P. J.; Lis, E.; Reiss, D.; Gibson, R. E.; Markowitz, M. K.; DiPardo, R. M.; Su, D.-S.; Bock, M. G.; Gould, R. J.; Pettibone, D. J. Generation and characterization of a human bradykinin receptor B1 transgenic rat as a pharmacodynamic model. *J. Pharmacol. Exp. Ther.* **2004**, *310* (2), 488–497.
- Gougat, J.; Ferrari, B.; Sarran, L.; Planchenault, C.; Poncelet, M.; Maruani, J.; Alonso, R.; Cudennec, A.; Croci, T.; Guagnini, F.; Urban-Szabo, K.; Martinolle, J.-P.; Soubrie, P.; Finance, O.; Le Fur, G. SSR240612 [(2R)-2-[(3R)-3-(1,3-benzodioxol-5-yl)-3-[(6-methoxy-2-naphthyl)sulfonyl]amino]propanoyl]amino]-3-(4-[[2R,6S]-2,6-dimethylpiperidiny]methyl]phenyl)-N-isopropyl-N-methylpropanamide hydrochloride], a new nonpeptide antagonist of the bradykinin B1 receptor: Biochemical and pharmacological characterization. *J. Pharmacol. Exp. Ther.* **2004**, *309* (2), 661–669.
- Wood, M. R.; Kim, J. J.; Han, W.; Dorsey, B. D.; Homnick, C. F.; DiPardo, R. M.; Kuduk, S. D.; MacNeil, T.; Murphy, K. L.; Lis, E. V.; Ransom, R. W.; Stump, G. L.; Lynch, J. J.; O’Malley, S. S.; Miller, P. J.; Chen, T.-B.; Harrell, C. M.; Chang, R. S. L.; Sandhu, P.; Ellis, J. D.; Bondiskey, P. J.; Pettibone, D. J.; Freidinger, R. M.; Bock, M. G. Benzodiazepines as potent and selective bradykinin B1 antagonists. *J. Med. Chem.* **2003**, *46* (10), 1803–1806.
- Su, D.-S.; Markowitz, M. K.; DiPardo, R. M.; Murphy, K. L.; Harrell, C. M.; O’Malley, S. S.; Ransom, R. W.; Chang, R. S. L.; Ha, S.; Hess, F. J.; Pettibone, D. J.; Mason, G. S.; Boyce, S.; Freidinger, R. M.; Bock, M. G. Discovery of a potent, nonpeptide bradykinin B1 receptor antagonist. *J. Am. Chem. Soc.* **2003**, *125* (25), 7516–7517.
- Marceau, F. A possible common pharmacophore in the nonpeptide antagonists of the bradykinin B1 receptor. *Trends Pharmacol. Sci.* **2005**, *26* (3), 116–118.
- Cannon, J. G. Analog design. In *Burger’s Medicinal Chemistry and Drug Discovery*, 5th ed.; Wolff, M. E., Ed.; John Wiley and Sons, Inc.: New York, 1995; Vol. 1: Principles and Practice, pp 788–791.
- Corey, E. J.; Bakshi, R. K.; Shibata, S. Highly enantioselective borane reduction of ketones catalyzed by chiral oxazaborolidines. Mechanism and synthetic implications. *J. Am. Chem. Soc.* **1987**, *109* (18), 5551–5553.
- Lautens, M.; Rovis, T. Selective functionalization of 1,2-dihydronaphthalenols leads to a concise, stereoselective synthesis of sertraline. *Tetrahedron* **1999**, *55* (29), 8967–8976.
- Flack, H. D. On enantiomorph-polarity estimation. *Acta Crystallogr., Sect. A* **1983**, *A39* (6), 876–81.
- Shannon, C. E. Prediction and entropy. *Bell Syst. Tech. J.* **1951**, 50–64.
- Sundaram, K.; Viswanadhan, V. N.; MacElroy, R. D. Information contained in protein shapes. *Int. J. Pept. Protein Res.* **1983**, *21*, 107–117.
- Viswanadhan, V. N.; Mattice, W. L. Assessment of bond rotation interdependence in polymer chains: An information theory approach. *Macromolecules* **1987**, *20*, 685–688.

JM061224G